MECHANICAL ASPECTS OF RESIDUAL STRESS DEVELOPMENT IN SHOT PEENING

S. T. S. Al-Hassani

Department of Mechanical Engineering, University of Manchester, Institute of Science and Technology, U.K.

ABSTRACT

Research on shot peening parameters has so far been of an experimental nature. In this lecture an attempt is made to highlight the main aspects of the process with a view to embracing a wide body of related phenomena which will assist in future analytical work. Shot peening is viewed as a multiple impact process. Interaction between shot and target is discussed and the sequence of events during the loading and unloading cycles which lead to residual stress development are examined. Attention is focused on single ball impact to obtain simple expressions for the depth of the plastic zone and how it is influenced by the velocity and density of the shot and the strength of the target. The theoretical expressions compare well with experiments. Further discussions are presented on the influence of strain rate and strain hardening and reference is made to concepts such as shakedown and Bauschinger effect.

KEYWORDS

Static; dynamic; plastic zone; P, S, H and Rayleigh waves; single and multiple impacts; prediction of residual stress distribution; strain rate; shakedown; Bauschinger effect.

INTRODUCTION

The response of a material to multiple impact by projectiles is a complex function of the physical properties of the target and projectile. When hard spherical projectiles impinge upon a target of elastic/plastic material and the impact velocity is sufficiently high, the target material undergoes local plastic deformation and, upon rebound, the rest of the elastic material tends to push the plastically deformed zone resulting in compressive stresses. Our prime concern in the shot peening process is to control the magnitude and subsequent distribution of these residual stresses.

It is now established that the impact of the shots causes plastic deformation with lateral stretching and grain distortion and upon elastic recovery the target acquires a shallow layer of superficial compressive residual stress below which it develops smaller equilibrating tensile stresses. Typical residual stress distri-

butions in thick and thin plate specimens are sketched in Fig. 1. Extensive experimental results on residual stress distributions under various conditions may be found in Flavenot and Nikulari (1977).

Thin plates normally curve upwards but thick blocks are too resilient to show any detectable curvature. Hard materials engender peak residual stress below the surface.

In the shot peening process the magnitude of the residual compressive stress at the uppermost layers and the depth to which the plastic deformation extends play a most significant role in the fatigue and stress corrosion performance of the peened component. That is why any significant contribution towards the control of the physical parameters of the process must aim at correctly predicting the residual stress distribution. To date, there has been an extensive amount of experimental work on Almen intensity, arc height development, residual stress measurements, fatigue life, etc. Notwithstanding, there is a noticeable lack in the literature of analytical work on shot peening. This is not surprising, however, due to the complex manner in which target materials respond to the multiple impact of shots. It is cumbersome enough to attempt to predict the impact response of a material to a single blow, as this would require fundamental understanding of high strain rate elastic as well as inelastic phenomena. The requisite understanding of single blow impact is still incomplete, but considerable progress has been achieved in recent years. The present level of comprehension is reviewed in the books by Goldsmith (1960) and Johnson (1972). This knowledge of high strain rate phenomena can be used to develop a physical description of the sequence of events that accompany the impact of a single projectile. When multiple impact takes place, the problem becomes more complex as it will require understanding of other aspects such as shakedown, progressive plastic deformation, Bauschinger effect and strain softening due to cyclic plastic deformation. Furthermore, the contact characteristics between thick target and projectiles and the concomitant stress waves will need to be examined.

In this lecture, an attempt is made to describe some of the important mechanical aspects of this rather intriguing and challenging process. Concern will mainly be focused on the development of highly simplified expressions in single impact situations which may be useful in relating parameters such as projectile density size and velocity and target hardness to thickness of the plastically deformed layer.

STATICAL ASPECTS

The elastic field below a concentrated load (P) acting on a semi-infinite surface is well known as the Boussinesq problem (1892). Fig. 2(a) shows the resultant stress σ at any point A given by $(3P/2\pi d^2)$ where d is the diameter of the circle and the stress will be directed towards (O) at all points. In a two-dimensional situation these circles will be lines of constant shear stress, see Shaw and DeSalvo (1970). Fig. 2(b) shows lines of maximum elastic shear stress beneath a smooth spherical indenter obtained from a Hertz analysis (see, for example, Timoshenko and Goodier (1951) or Davies (1949). The load distribution is hemispherical and the ratio of mean $\bar{p}$ to maximum p_o pressure is 2/3. The maximum shear stress τ lines represent non-dimensionalized values of $\tau/\bar{p}$. Fig. 2(c) is a plot of $\tau/\bar{p}$ versus the non-dimensional distance below the surface Z/a from the vertical centre line. The base of the punch is drawn flat for convenience even though it is a spherical surface of a larger radius.

Plastic deformation will first occur at a point Z = 0.47a below the surface, corresponding to $\tau = 0.468\bar{p}$. Using maximum shear Tresca yield criterion, the stress at this point is 0.5Y and thus $\bar{p} = 1.07Y$. As the load is increased, the plastic flow zone will grow and extend to the surface of the punch.

Plastic Zone

By the maximum shear criteria, one of the lines of maximum shear stress in Fig. 2(b) should correspond to the plastic-elastic boundary for fully developed plastic flow.

In the fully plastic state where the elasticity of the medium is ignored and the theory of rigid plasticity applies, slip line solutions are used to identify the regions of velocity discontinuities along which material flows towards the surface. Normally, two-dimensional solutions are applied. Two famous slip line solutions are due to Prandtl (1920), Fig. 3(a), and to Hill (1950), Fig. 3(b). The depth of the plastic flow in the Prandtl's case is 1.414a whilst that in the Hill's case is 0.707a. Experiments on ball indentation of thick blocks, however, reveal different values and indeed show a plastic zone which is contained by the elastic field surrounding it, see, for example, Samuels and Mulhearn (1957) and Shaw and DeSalvo (1970). The plastic boundary can be fairly represented by a curve which closely fits a Hertz maximum shear line more than a slip line as sketched in Fig. 3(c). In fact, our experiments reveal that the plastic boundary in dynamic indentation also has a similar shape as shown in Fig. 3(d).

The problem of determining the depth of the plastic zone in elastic-plastic axisymmetric flow is discussed by Shaw and DeSalvo (1970). By matching the Hertz solution with that of the Boussinesq problem, they obtain an equivalent concentrated loading situation from which the required maximum shear stress contour which defines the plastic boundary is obtained. The analysis is involved and beyond the scope of this report. The depth of the plastic boundary was theoretically predicted to be $h_p = 1.816a$ below the surface corresponding to a $\tau/\bar{p}$ value of 0.177 in Fig. 2(b). In terms of the radius of the spherical indenter R and the depth of indentation $\bar{Z}$, this become (assuming $a^2 \simeq 2\bar{Z}R$),

$$\frac{h_p}{R} = 2.57\left(\frac{\bar{Z}}{R}\right)^{\frac{1}{2}} . \qquad (1)$$

The 0.177 contour corresponds to $\bar{p} \simeq 2.82Y$ (for $\tau = 0.5Y$) which requires a maximum constant pressure at the centre of the contact surface of 3/2 x 2.82Y = 4.23Y. After allowance for contour distortions near the edges of the indenter, a factor of 0.94 is predicted for correcting the value of $\bar{p}$ to become 2.82/0.94 = 3.0Y which is close to experimental values.

It may well be worth remembering that in shot peening we are dealing with more than one axisymmetric indentation and therefore the equivalent two-dimensional problem could offer a better value! In this case the depth of the plastic zone is 2.99a or $\frac{h_p}{R} = 4.23\left(\frac{\bar{Z}}{R}\right)^{\frac{1}{2}}$.

Residual Stress after Load Removal

We now consider the mechanics of residual stress development on removal of the spherical indenter. Consider an element at point A on the vertical centre line within the plastic boundary, Fig. 3(c). The action following the application of the external load may be considered, as suggested by Shaw et al (1970), in two steps. In the first, the elastic stress field σ_1 and σ_2 will be fully developed as load P is applied, but plastic flow will not have occurred, Fig. 4(a). When

plastic flow occurs, stresses H_1 will develop in the two transverse directions, Fig. 4(b). Flow will continue until the Tresca yield criterion is satisfied, and thus

$$\sigma_1 - H_1 = Y \tag{2}$$

On removal of the external load, σ_1 will vanish and the state of stress will be as shown in Fig. 4(c) provided H_1 does not exceed Y. If $H_1 > Y$ then a second plastic flow (or reversed yielding) will occur on unloading and stress H_2, Fig. 4(d), will develop where

$$H_2 = H_1 - Y \tag{3}$$

in accordance with the Tresca yield criterion.

The plastic material beneath an axisymmetric indenter can contain residual compressive stresses that are much higher than Y. For example, at the centre of the top surface $\sigma_1 = 4.23$ so that the maximum lateral residual stress is $H_1 = 3.23Y$ for a Hertz-type load distribution.

Elastic-plastic stress analysis by classical continuum mechanics becomes intractable. While the above analyses depended on certain simplifying assumptions, the finite element method can yield numerical results with great accuracy. Such a study on elastic, perfectly plastic materials was made by Hardy etal (1971). Inclusion of strain hardening as well as inertia effects are at present the subject of investigation by Al-Obeid in our Department.

In shot peening, the far field stress due to one indenter adds to the stress below the other indenter if load application occurs simultaneously. Consequently, plasticity may be reached earlier and the plastically deformed depth may tend to be slightly shallower. However, in practice, the occurrence of impact is random and also includes multiple single as well as repeated impacts. The plastic zones below the shots join together to form an upper layer of residual compressive stress almost uniform over the active surface of the medium.

The plastic indentation of metals was studied by Tabor (1951) in static and dynamic conditions. Interestingly, he found that, due to elastic recovery, the indentation rebounds to a shallower curvature after being deformed. This shallowing effect of each indentation when integrated all over the surface of a shot peened plate manifests itself in the form of an upward curvature producing the conventional arc height in an Almen strip. The arc height continues to increase as the surface is progressively covered and repeatedly impacted until a stage is reached when no more curvature is produced by the imparted energy and the component is said to have reached saturation. There is much to be propounded on how saturation is reached. Speculative reasons are given when discussing influence of strain rate, strain hardening, shakedown and Bauchinger effect.

DYNAMICAL ASPECTS

As above, we consider the aspects in a single impact first. The problem of an elastic sphere striking a semi-infinite solid of the same material is commonly solved by resort to the Hertz contact "force-approach" expression and assumed to be the decelerating force acting on the projectile (see, for example, Timoshenko and Goodier (1951). For a density of material ρ, Poisson's ratio ν and Young's modulus E, a projectile of radius R impinging upon the surface with a velocity V produces a maximum average pressure given by

$$\bar{P} = \frac{2}{3\pi}(2.5\pi\rho)^{1/5}\left[\frac{E}{1-\nu^2}\right]^{4/5} V^{2/5} \qquad (4)$$

and the duration of impact, $\bar{t}$, is given by,

$$\bar{t} = 2.943\left[2.5\pi\rho\left(\frac{1-\nu^2}{E}\right)\right]^{2/5}\frac{R}{V^{1/5}} \qquad (5)$$

For a steel ball of 6.36 mm diameter dropping from 10 m height onto a steel block, we have a strikingly high value of $\bar{p}$ = 4.0 MN/m^2 (260 ton/in^2) and $\bar{t}$ = 16.7 μ sec. In practice, of course, the deformable material of the target and the projectile have inertia and, consequently, stress waves are generated in both and for any study on the dynamical aspects to be of practical value, these stress waves must be examined.

There is an enormous amount of literature on stress waves in semi-infinite solids. Some of those of direct relevance to the present problem are authored by Tsai (1968), Ching-Hsie Yew and Goldsmith (1964), Kolsky (1963), Engel (1976), Hopkins (1960), Lamb (1904) and Goodier et al (1959).

It is now fairly established that when a spherical projectile impinges upon a surface, part of the kinetic energy is converted into strain energy which is propagated from the point of impact into the interiors and surfaces of both the projectile and the target. This energy is manifested in the form of travelling stress waves and the properties of these in turn are governed by material and geometrical properties of the medium.

In an elastic target, two kinds of waves are propagated through the interiors of the medium. A dilatational wave or a Push-Pull (P wave) which travel at the speed $[(\lambda + 2\mu)/\rho]^{1/2}$ and a rotational or distortional shake wave (S wave) which travels at the speed $(\mu/\rho)^{1/2}$ where λ and μ are the Lame constants and ρ the density. The wave fronts of these waves are shown in Fig. 5(a).

Another type of elastic wave of importance to impact problems is a surface or (Rayleigh) wave. These mainly travel over the surface and therefore carry a large proportion of the energy to much larger distances than P or S waves. Due to the grazing incidence of the P wave on the stress-free surface, another shear type wave called Head or (H) wave is also generated as shown. A surface strain record at a position near the impact zone would look as depicted in Fig. 5(b). The faster strains of the P wave first arrive, next those of the S wave and lastly the large amplitude R wave.

If the projectile was soft, the rate at which the contact circle expands could interact with the Rayleigh wave. Such a phenomenon is of vital interest in the field of erosion due to water impact, Salem et al (1979), and also in the field of explosive welding where the interfacial waves between the impacter and the target plates have to be controlled, see, for example, Salem and Al-Hassani (1981). On the other hand, if the projectile was rigid and the target can offer plasticity, a plastic wave will spread from the impact point with a velocity given by Hopkins (1960) as

$$c_p^2 = \frac{K}{\rho}\left[\frac{1 + H'(\varepsilon)/3K}{1 - H'(\varepsilon)/9K}\right]$$

where K is the bulk modulus and $H'(\varepsilon)$ the tangent modulus derived from the plastic stress-strain relation $\sigma = Y + H(\varepsilon)$ where Y is the uniaxial yield stress.

Plastic waves are slower than elastic waves. Consequently, when unloading occurs, elastic unloading waves quickly catch up with the plastic waves generated earlier in the pressure cycle. It has been demonstrated by White (1949) that "internal reflections" occur at the plastic wave front in work hardening materials; an elastic wave is propagated back towards the surface and a plastic wave of reduced amplitude continues to propagate into the material and so on until all plastic action is diminished and only elastic waves remain circulating within the body. Unloading of the plastically deformed region behind the plastic wave front can also occur due to the arrival of tensile elastic waves returning after reflection from the free boundaries. In fact, these reflected waves could be so severe that in brittle materials they cause spalling fractures. It is also important to note that in solids of curved boundaries, e.g. the projectile, the reflected waves focus within the body and cause internal fractures. A typical fractured sphere of perspex subject to a fast blow is shown in Fig. 6. This is of relevance to the study of the behaviour of glass and ceramic beads during impingement. For further details on the subject of stress wave focus sing and fracture, see Silva Gomes and Al-Hassani (1977).

Normally, components to be shot peened are thin and the shots are small and hard. Consequently, the transit time of stress waves is much shorter than the contact duration. Many elastic wave traverses may take place before the shot bounces back. In the meantime, the plastic zone develops below the projectile. Our experiments have shown a great similarity between the shape of the plastic zones obtained by impact and by static indentation. Indeed, the depth of the plastic zone is nearly equal in both cases provided the indentation is of the same extent. This discovery enables us to use equation (1) with reasonable confidence. In Fig. 7, this equation is compared with results obtained from static indentation tests and dynamic tests. The dynamic tests were performed using a specially designed Tornedo cartridge gun with velocity measuring facility as shown in Fig. 8. Steel spheres of 4.8 mm diameter were projected on steel targets with velocities in the range 50 to 150 m/sec. Further details on the instrumentation may be had from Tabai (1981).

Repeated impacts on the same spot confirmed the findings of Pope and Mohamed (1955) in that the plastic zone spreads gradually, but our results revealed that there is an extent beyond which no further spread will occur without further increase of the impact energy level, see Fig. 9(a) for repeated impact at 75 M/Sec.

Another interesting experimental feature is that when additional impacts are caused to occur adjacent to each other, the plastic zones join up to form a uniform plastic layer as shown in Fig. 9(b). This is also found in static indentation tests.

So, it is fair to assume that in the range of impact conditions pertaining to shot peening, the plastic zone well develops before unloading waves diminish it away. This is also confirmed by a numerical computation (Evans et al 1978). During the plastic action, the contact pressure distribution may justifiably be assumed similar to that commensurate with the static indentation. This holds reasonably well if target inertia was negligible. In such situations, we can use the value of $\bar{p} = 3Y$ for the average resisting dynamic pressure to the projectile. If, however, target inertia was important, then stress waves must be accounted for. To simplify such situations we may choose to neglect elastic waves, Hutchings (1979). Here, the contact characteristics can be approached from the dynamic solutions for an expanding pressurized cavity, see Fig. 10(a) Such solutions identify the equation of motion for a cavity of radius r_o as Goodier (1965),

$$\frac{\partial \sigma_r}{\partial r} + \frac{2(\sigma_r - \sigma_\theta)}{r} = \rho \alpha \quad , \quad \alpha(r,t) = \frac{r_o^2 \ddot{r} + 2 r_o \dot{r}_o^2}{r^2} - \frac{2 r_o^4 \dot{r}_o^2}{r^5} \quad , \qquad (6)$$

where α is the particle acceleration at distance r from the centre. These equations are very similar to those for a thick wall sphere subjected to an impulsive internal pressure, see Al-Hassani and Johnson (1969).

The solution to the above equation is expected to be only useful near the central axis if the projectile wherein r_o is equated to the projectile radius R and $\dot{r}_o$ to the penetration rate. Following this analysis, we may arrive at an estimate of the average strain undergone by the target. In an expanding thick sphere, the radial strain rate at distance r is $\dot{\varepsilon}_r = \frac{2VR^2}{r^3}$ and the hoop strain rate is $\dot{\varepsilon}_\theta = \frac{-VR^2}{r^3}$ where V is the radial velocity of the inner wall. Hence the representative strain rate $\dot{\bar{\varepsilon}} = \sqrt{\frac{2}{3}[2(\dot{\varepsilon}_r - \dot{\varepsilon}_\theta)]} = 2\dot{\varepsilon}_\theta$ which at the expanding surface becomes 2V/R. The final strain rate is zero and hence the average value may be considered to be V/R which, for V = 80 m/sec and R = 2.38 mm, gives 3.4×10^4/sec. This shows that in high speed shot peening the strain rate is of considerable importance as steel can triple its yield stress at such high rates.

In low velocity shot peening, i.e. shallow penetration situations, the above equations do not hold and the problem becomes intractable. However, it may be justified to ignore inertia effects in such circumstances and a quasi-static type analytical approach may be employed as follows:-

The equation of motion of a spherical projectile decelerated by an average pressure $\bar{p} = 3Y$ (assumed constant) may be

$$M \frac{dv}{dt} = - \pi a^2 \bar{p} \qquad (7)$$

where M is the projectile mass $= \frac{4}{3}\rho\pi R^3$ and a is the contact radius.

The equation may be integrated in terms of the penetration (assumed to be small $\simeq a^2/2R$) to give,

$$\frac{\bar{Z}}{R} = \left(\frac{2}{3}\right)^{\frac{1}{2}} \cdot \left(\frac{\rho V^2}{\bar{p}}\right)^{\frac{1}{2}} \qquad (8)$$

where $\bar{Z}$ is the final indentation and V is the initial impact velocity.

The non-dimensional number $(\rho V^2/\bar{p})$ comes in most impact problems. It gives a measure of the severity of impact and is sometimes called the "Damage Number". It may be used to identify dynamic similitudes in shot peening situations in a similar manner to that used in small scale testing of vehicles under crash conditions, see Lowe et al (1972) and Johnson (1972). In this way, shot peening of an Aluminium component can be compared with another of steel. Equation (8) is compared with results from dynamic tests on single impact as shown in Fig. 10a. The target material was mild steel and the projectiles were hard ball bearings with R = 2.38 mm. The agreement is seen to be encouraging. The value used for Y is 70×10^3 psi which is on the low side being at low strain rate and a better agreement between theory and experiment would be obtained if higher values were used.

Depth of Plastic Zone

Now, by assuming that quasi-static conditions still hold in the range of impact velocities and thus dynamic indentations which have the same value as those obtained from static tests produce similar plastic zones, Fig. 7, we combine equation (8) with equation (1) and get the depth of the plastic zone as

$$\frac{h_p}{R} = 2.57\left(\frac{2}{3}\right)^{\frac{1}{2}}\cdot\left(\frac{\rho V^2}{\bar{p}}\right)^{\frac{1}{2}} \tag{9}$$

which is a most useful relationship for relating shot peening parameters.

Comparison between values of h_p obtained from etching steel specimens subjected to single impact tests with the predictions of this equation are given in Fig.11(b). Eqn. (9) is also found to compare well with the experimental results of Meguid et al (1976) obtained from actual shot peening tests on steel specimens.

This theoretical relationship reveals that the depth of the plastic zone increases with shot size, density and velocity and decreases with the hardness of the target.

To allow for work hardening effect we may use Meyer Indentation Law, Goodier (1965) which relates the resisting pressure to the contact radius by

$$\bar{p} = \bar{p}_y\,(a/R)^n \tag{10}$$

where n is a constant related to the work hardening exponent and p_y is a measure of the plastic flow stress. The previous equation of projectile motion will then be modified and the result becomes

$$\frac{\bar{z}}{R} = \left[\frac{(4+n)}{6\times 2^{n/2}}\cdot\left(\frac{\rho V^2}{\bar{p}_y}\right)\right]^{2/4+n} \tag{11}$$

and the effective depth of the plastic zone will then be

$$\frac{h_p}{R} = 2.57\left[\frac{(4+n)}{6\times 2^{n/2}}\cdot\left(\frac{\rho V^2}{\bar{p}_y}\right)\right]^{1/4+n} \tag{12}$$

For a non-hardening material, n = 0 and we get equation (9) again.

Justification of using Meyer's equation (10) for strain hardening contact problems is given by Halling and Nuri (1975).

To allow for both the strain hardening and rate effects, we propose a Meyer Indentation Law such that equation (10) has a form, corresponding to $\sigma = B\varepsilon^n\dot{\varepsilon}^m$,

$$\bar{p} = A\,(a/R)^n\,(\dot{a}/R)^m \tag{13}$$

where $A\,(\dot{a}_r/R)^m = \bar{p}_{yr}$ the plastic flow pressure at a reference (e.g. quasi-static) indentation rate V_r and m is a constant related to the strain rate index.

Solution of equation (7) with p from (13) now gives

$$\frac{\bar{Z}}{R} = \frac{1}{2}\left[\frac{4}{3}\ \frac{4+n-m}{2-m}\cdot\left(\frac{V_r}{V_o}\right)^m\cdot\left(\rho\frac{V_o^2}{\bar{P}_{yr}}\right)\right]^{2/(4+n-m)} \qquad (14)$$

which clearly shows that for high speed impacts $V_r > V_o$, the indentation and hence the plastic zone becomes shallower.

For example, for a material with n = m = 0.25, the value of $\bar{Z}$ will be 0.34 and 0.58 times those corresponding to the case when m = n = 0. There are materials which, at certain conditions of heat treatment, become only strain rate sensitive. These are called superplastic materials like Zn-Al alloys, Al-Hassani et al (1977), which possess a large value of m but with n = 0. It should be most interesting to examine the shot peening behaviour of superplastic alloys.

In the shot peening industry, the impact velocity of the shot is not measured. Instead, the R.P.M. of the wheel in a wheel type machine or the air pressure in a jet type machine are used. In the case of the wheel, it is a simple matter to relate the peripheral velocity of the shot to the wheel R.P.M. In jet blasting, a relationship of the type found in fluid mechanics, $P_p = kV^{\beta}$, between the peening pressure P_p and the downstream velocity of the shots, V, could well be used. The constant k depends upon the nozzle dimensions and shot size and density whilst β is an exponent more dependent upon the flow characteristics of the air-stream. It is expected that values of k and β would vary from one system to another, but it should be a simple exercise to establish a table of values to go with each machine.

A useful formula for the industrialist may therefore be obtained by substituting for V in terms of P_p in any of equations (9) to (14). For example, equation (9) becomes,

$$\frac{h_p}{R} = 2.57\cdot\left(\frac{2\rho}{3\bar{p}}\right)^{1/4}\cdot\left(\frac{P_p}{k}\right)^{2/\beta} \qquad (15)$$

A typical value for β may be $\simeq$ 0.5 and the equation becomes

$$\frac{h_p}{R} = 2.57\cdot\left(\frac{2}{3}\right)^{1/4}\cdot\left(\frac{\rho}{k}\right)^{1/4}\cdot\left(\frac{P_p}{\bar{p}}\right)^{1/4}$$

which indicates that the peening pressure increases the plastic zone whilst the hardness, $\bar{p}(\simeq 3Y)$, tends to decrease it in much the same degree of influence.

Now that we have obtained simple expressions for the depth of the plastic zone, we are in a position to consider the residual stress distribution in an actual shot peening operation.

RESIDUAL STRESS DISTRIBUTION

It is now established that under each impact spot there will be a plastic zone constrained by an elastic field. After rebounce of each shot the plastic zone interacts with the elastic field resulting in a residual stress distributed through the depth of the component. The retained plastic zone resembles a nail pushed into a block of wood. The retaining forces come from the reluctance of the indented material to be moved within the block and thus engender normal and tangential frictional forces which keep the nail in position, see Salem et al (1975).

As the stream of shots repeatedly and progressively impinges upon the surface, more and more plastic zones are created until all join up to form an almost uniform plastic layer of thickness h_p. The local strains produced by each impact interact with one another to produce a final average value over the entire surface, so that the end state of stress is produced as a result of the integrated effect of a progressive action rather than an instantaneous action over the entire surface.

There has been a tendency in the shot peening literature, Al-Obeid et al (1981), to interpret the residual stress in the component as if it were a result of a stretching action, uniformly and instantaneously distributed over the surface followed by an elastic unloading action again distributed uniformly over the entire length of the specimen. Consequently, simple beam and plate bending theories are then used to explain the general features of the process. In addition to the neglect of the history of the residual stresses, such a concept relies on a major assumption that plane sections in the plate remain plane. Due to the very local nature of the plastic deformation, the last assumption seriously departs from physical reality. However, such concepts are quite efficient when used in interpreting arc height variation due to the removal of top surface layers.

In order to circumvent the problem of local plasticity and still use simple plate bending theory, Flavanot and Nikulari (1977) conceived what they called a "stress source" to exist in the material so as to balance the bending and axial stresses which are produced by the whole body of the plate as it tends back to its original undeformed state. They assumed the function of this stress to be the same as that of the residual stress engendered in a very thick block, see Fig. 3(a), so the residual stress distribution in a thin plate, see Fig. 1(a), is the result of further addition of the bending and axial stresses, i.e.

$$\sigma_R(Z) = \sigma_{bending} + \sigma_{axial} + \sigma_s \tag{16}$$

From experimental evidence, the shape of the residual stress distribution in a thick target, Fig. 1(a), can be represented by a cosine function. By considering the source stress σ_s to be "elastic" they proposed the form $\sigma_s = - E \varepsilon(Z)$ where E is the Young's modulus and

$$\varepsilon(Z) = \varepsilon_m \cos\left(\frac{\pi Z}{2h_p}\right) \left[1(h_p)\right] \tag{17}$$

when Z is measured from the top surface and the Unit Heavyside function $\left[1(h_p) = 1 \text{ for } 0 \leq Z \leq h_p \text{ and } = 0 \text{ for } Z > h_p\right]$ is introduced by the present author to indicate that the function is only valid up to $Z = h_p$. This function has a peak at the top surface and in order to allow for the peak to occur at a distance αh_p below the surface, see Fig. 1(a), they shifted the curve to obtain,

$$\varepsilon = \varepsilon_m \cos \pi \left[\frac{Z - \alpha h_p}{2(1 - \alpha)h_p} \right] \tag{18}$$

The bending stress at depth Z in a beam of width b and thickness h subject to a bending moment $\bar{M}$ is given by $\frac{12\bar{M}}{bh^3}\left(\frac{h}{2} - Z\right)$ where

$$\bar{M} = \int_0^h \sigma(Z) \cdot \left(\frac{h}{2} - Z\right) \cdot b \cdot dZ \tag{19}$$

Similarly, the axial stress is given by $\frac{\bar{F}}{bh}$ where

$$\bar{F} = \int_0^h \sigma(Z) \cdot b \cdot dZ \qquad (20)$$

Flavenot and Nikulari used $E\varepsilon(Z)$ for $\sigma(Z)$ and integrated (19) and (20) over $0 \leqslant Z \leqslant h_p$ and then substituted in equation (16) to obtain the residual stress distribution as

$$\sigma_R(z) = E\varepsilon_m \left[\frac{12}{\pi h}(1-\alpha)\left(\frac{h}{2}-Z\right)C_1 + \frac{2\lambda}{\pi}(1-\alpha)C_2 - \frac{\varepsilon(z)}{\varepsilon_m}\right], \qquad (21)$$

where $\lambda = h_p/h$ (22)

$$C_1 = 1 - 2\lambda + \frac{4\lambda}{\pi}(1-\alpha)\cos\frac{\pi\alpha}{2(1-\alpha)} + \sin\frac{\pi\alpha}{2(1-\alpha)} \qquad (23)$$

and $C_2 = 1 + \sin\frac{\pi\alpha}{2(1-\alpha)}$ (24)

The value of ε_m is obtained by consideration of plane sections remaining plane in a beam of length L bent into an arc height, δ, and expressing the curvature by $\bar{M}/EI$. The expression obtained is

$$\varepsilon_m = \frac{2}{3}\,\frac{\pi h \delta}{\lambda^2 L^2 h_p (1-\alpha) C_1} \qquad (25)$$

Despite the latter assumption in obtaining equation (25), the agreement between equation (21) and experimental results was found to be very good. This is, of course, expected since in the first place one has to use an experimentally obtained function, viz. dquation (18). The limitations of this analysis lie in the need for knowledge of h_p, α and δ à priori. The importance of equation (9) above now becomes clear. By substituting for h_p from (9) into equation (22) we get

$$\lambda = 2.57 \cdot \left(\frac{2}{3}\right)^{\frac{1}{4}} \cdot \left(\frac{R}{h}\right) \cdot \left(\frac{\rho V^2}{\bar{p}}\right)^{\frac{1}{4}} \qquad (26)$$

which makes equation (21) most valuable in predicting the residual stress distribution from knowledge only of the arc height, for situations with $\alpha = 0$, and shot density ρ, velocity V and size R as well as the hardness $\bar{p}$. To evaluate all these parameters we do not require metallurgical inspection.

It is worthwhile to point out that the residual stress is not defined uniquely by the arc height. A knowledge of h_p is also required, so that one expects a family of residual stress functions to give the same arc height. This is a startling aspect as the whole of shot peening practice is based on classifying the intensity by means of the arc height above.

Spherical Model

A more realistic, although rather rudimentary, analysis may be suggested here. In order to avoid using the assumption of plane sections remaining plane during the loading cycle and to allow for future inclusion of statistical summation of multiple progressively produced indentations, we envisage that the stress field below each dent may be represented, as suggested earlier, by that commensurate in

an elastic/plastic medium containing a spherical cavity, see Fig. 10(a). Assuming that quasi-static conditions hold, i.e. ignoring the term $\rho \ddot{\alpha}$ in equation (6), the radial σ_r and hoop σ_θ stress distributions in a thick sphere of outer radius b with its inner cavity radius R pushed such as to establish a plastic zone extending to a radial distance r = C is given by

$$\frac{\sigma_r}{Y} = -2 \ln\left(\frac{C}{r}\right) - \frac{2}{3}\left(1 - \frac{C^3}{b^3}\right) \qquad R \leq r \leq C \qquad (27a)$$

and

$$= \frac{\sigma_\theta}{Y} - 1$$

$$\frac{\sigma_r}{Y} = -\frac{2}{3}\frac{C^3}{b^3}\left(\frac{b^3}{r^3} - 1\right)$$

and

$$C \leq r \leq b \qquad (27b)$$

$$\frac{\sigma_\theta}{Y} = \frac{2}{3}\frac{C}{b^3}\left(\frac{b^3}{2r^3} + 1\right)$$

These equations may be found in any plasticity text and are sketched in Fig. 10(b) with the plastic zone depth h_p defined by C - R.

It is seen that the curve describing σ_θ, which is the one of interest in our problem, gives a peak at $r = h_p$. This is more realistic than that suggested by the stress-source method. The special feature of this expression is that it incorporates both plastic and elastic stresses.

We can transform this distribution into the plate configuration such that all the spherical plastic zones under the spherical dents join up and resist the bending and axial forces of the plate as it tends to retain its original unbent shape. Let b - R = h, r - R = Z, $\sigma_\theta = \sigma(Z)$ and C - R = h_p, the above distribution becomes

$$\frac{\sigma(Z)}{Y} = 1 - 2\ln\left(\frac{h_p + R}{Z + R}\right) - 2\left[1 - \left(\frac{h_p + R}{h + R}\right)^3\right], \quad 0 \leq Z \leq h_p \qquad (28a)$$

and

$$\frac{\sigma(Z)}{Y} = \frac{2}{3}\cdot\left(\frac{h_p + R}{h + R}\right)^3 \cdot \left[\frac{1}{2}\left(\frac{h + R}{Z + R}\right)^3 + 1\right], \quad h_p \leq Z \leq h. \qquad (28b)$$

Now, if each spot unloads independently as if it were part of a spherical cavity, a residual stress distribution similar to that found in a spherical shell develops. This is sketched as $\sigma_{R\theta}$ in Fig. 10(c). The expression for $\sigma_{\theta R}$ may be found in texts, e.g. Kachanov (1974) and Johnson and Mellor (1962).

If, on the other hand, the unloading is assumed to take place by a whole plate action as in the case of equation (16), then by substituting for $\sigma(Z)$ from equation (28) into equations (19) and (20) to obtain the retaining $\bar{M}$ and $\bar{F}$ and then use them to elastically unload the elastic/plastic $\sigma(Z)$, we get a modified expression for $\sigma_R(Z)$ as

$$\sigma_R(Z) = \sigma(Z) - \frac{12\bar{M}}{h^3 b}\left(\frac{h}{2} - Z\right) - \frac{\bar{F}}{bh} \qquad (29)$$

with $\sigma(Z)$ from equations (28a) and (28b),

$$\frac{\bar{M}}{Y} = h_p\left(\frac{h}{2} + R\right) - R(h+R)\ln\left(1+\frac{h_p}{R}\right) + \frac{h_p}{3}(h - h_p)\left[1 - \left(\frac{h_p + R}{h + R}\right)^3\right] -$$

$$\frac{1}{12}\left\{\left(\frac{h_p + R}{h + R}\right)^3\left[(h+R)(3h+2R) - 4h_p(h - h_p)\right] + (h - 2R - 4h_p)^2\right\} \tag{30}$$

and

$$\frac{\bar{F}}{Y} = 2R\ln\left(1+\frac{h_p}{R}\right) - \frac{4}{3}h_p + \frac{1}{6}\left(\frac{h_p + R}{h+R}\right)^3(3h - R) + \frac{1}{6}(h_p + R) \quad . \tag{31}$$

For $h \gg h_p$ and R, equations (30) and (31) simplify to

$$\frac{\bar{M}}{Y} \simeq \frac{5}{6}h_p h - hR\ln\left(1 + \frac{h_p}{R}\right) - \frac{(h_p + R)^3}{3h} \tag{32}$$

and

$$\frac{\bar{F}}{Y} \simeq \frac{h_p + R}{6} - \frac{4}{3}h_p + 2R\ln\left(1 + \frac{h_p}{R}\right) + \frac{(h_p + R)^3}{2h^2} \quad . \tag{33}$$

With h_p/R from equation (9), it is possible to obtain a residual stress distribution directly from the impact parameters. This is most useful to the designer of shot peening. However, it is still limited in the sense that the curves obtained have a sharp kink at the transition between elastic and plastic zones due to neglect of hardening.

By putting $\sigma_R(Z) = 0$ we can obtain the transition depth between compression and tension. This analysis does not produce a peak residual stress below the surface. However, in practice the local spots unload individually and the sphere equations may still be used to predict a condition of reversed yielding, see Fig. 10(d). This is more in line with arguments presented in Fig. 4 and does produce a peak below the surface.

Reversed plasticity condition occurs in thick walled spheres, i.e. $b/R > 1.7$, whenever the sphere is unloaded after being loaded by a pressure exceeding the full plastic limiting pressure. Since in our particular indentation problems we are dealing with effectively very large b/R, it is possible that in many situations reversed yielding takes place on unloading.

Aspects of Repeated Loading

When each spot undergoes repeated impact the material in the plastic zone will pass through the stress and strain curve cyclically. If during each subsequent impact the material is subject to the combination of residual and contact stresses, which together may not reach the yield point, the system is said to "shakedown" to a resultant state of stress which is entirely elastic. If the applied stresses exceed the "shakedown limit", cumulative plastic flow will occur. This aspect, as applied to repeated passage of rollers over an elastic-plastic medium, is discussed fully by Merwin and Johnson (1963).

Shakedown seems to have much relevance to our problem, particularly when interpreting the saturation curves in Fig. 9(a) and of arc height versus time. When shakedown occurs in a sphere or a cylinder, they behave as if they were hardened in compression with their first loading. This phenomenon is known as "autofrettage". For severe impact conditions, however, the loads exceed the shakedown

limit and the material of each spot undergoes cyclic plastic straining which can cause work softening or plastic fatigue. A similar action in practice is found in the rapid failure of a wire under reversed plastic bending. In shot peening, exceeding this limit will obviously enhance erosion, Engel (1976).

High frequency repeated impact can give rise to a high local temperature. The temperature may reach a high enough value that the material tends to soften and if conditions are favourable the softening rate can predominate over the effects of the hardening rate. Such work softening may well be taking place in the layers near the surface; this perhaps explains the reason why the peak residual stress occurs below the surface.

Another aspect which is also of relevance to our problem is the "Bauschinger effect". This is due to the fact that strain hardening is usually directional in character. As a result of plastic deformation, the material therefore acquires a so-called strain-anisotropy. One of the manifestations of this is the Bauschinger effect which in fact is that previous plastic deformation decreases the resistance of the material to subsequent plastic deformation of opposite sign, Kachanov (1974).

The above aspects have been qualitatively presented. There is much to be desired in obtaining quantitative models to relate these to shot peening conditions. We are only just entering the world of mechanics of shot peening!

A final comment is now made on the aspect of saturation time. It is interesting to note that the equation of motion (7) can give a relation between the kinetic energy of the projectile and the volume, $\bar{V}$, of the indentation. The relation is

$$\frac{1}{2} M V_o^2 = \bar{p} \bar{V} \tag{34}$$

where $\bar{V} \simeq \pi a^4/4R$ (35)

The mass flow rate is given by NM where N is the number of shots per second. The energy imparted to the target per second is $\frac{1}{2}$ NM V_o^2. Thus, the rate at which volume of dents created by progressively impacting the surface is

$$\dot{\bar{V}} = \frac{NM V_o^2}{2\bar{p}} \tag{36}$$

Therefore, at time t, the volume of material shifted which is a measure of the increase in the surface area and also an indirect measure of the arc height is

$$\bar{V} = \left(\frac{NM V_o^2}{2\bar{p}}\right) t \tag{37}$$

In practice, N, M and V_o are constant. Equation (37) indicates that if $\bar{p}$ does not change due to multiple impacts, i.e. with time, then $\bar{V}$ (and consequently the arc height) will continue to increase linearly with time. However, repeated impact obviously increases $\bar{p}$ as manifested in the reduction of increments in $\bar{Z}$ and h_p with further impacts, Fig. 9(a). The manner in which p increases is naturally governed by the aspects discussed above, but it is fair to say that, whether due to strain hardening, strain rate or shakedown, the volume of $\bar{p}$ tends to increase further and further and thus the gradient of the line described by equation (37) will consequently decrease with time producing a curve resembling that of saturation. Equation (37) also shows that a steeper curve, and hence faster saturation, may be had by high velocity shots and high mass flow rate.

CONCLUDING REMARKS

The mechanics of shot peening present an exciting challenge to the scientist. It is a hybrid process involving many disciplines of static and dynamic elasticity and plasticity. In this paper, special attention is given to aspects of static and dynamic behaviour of a target impinged upon by a single sphere. After establishing the thickness of the plastic zone, it is assumed to hold for the entire body of target when subjected to repeated progressive impingement. Useful expressions are found from a rudimentary analysis for predicting the residual stress distribution. The limitations introduced by assuming plane sections remain plane in conventional analyses are avoided by introducing a new model of spherical cavity expansion. The resulting expressions relate the easily measurable impact parameters to the residual stress without having to resort to metallurgical inspection. An attempt is made to explain the concept of saturation by reference to "shakedown", "Bauschinger effect", "strain hardening" and "strain rate". There is still a huge lack of knowledge. We are only just entering the area of mechanics of shot peening.

ACKNOWLEDGEMENTS

The author would like to express his sincere thanks to Mr. A. Tabei for assistance in the experimental work and to Dr. J. Kettlewell and Mr. Y. Al-Obeid for their useful comments and suggestions.

REFERENCES

Al-Hassani, S.T.S., Clemas, G.G.W. and Al-Naib, T.Y.M. (1977). "The free bulge forming of Zn-Al superplastic sheet from a circular die". Proc. 18th Int. Machine Tools Design & Research Conf., London, Sept. McMillans.

Al-Hassani, S.T.S. and Johnson, W. (1969). "The dynamics of the fragmentation process for spherical shells containing explosives". Int. J. Mech. Sci., 11, 10, p.811.

Al-Obeid, Y. "Finite element approach to shot peening mechanics". Ph.D. Thesis to be submitted to Univ. Manchester.

Al-Obeid, Y. and Al-Hassani, S.T.S. (1981). "A critical survey of literature on shot peening". To be published.

Boussinesq, J. (1892). "Application des Potentials". Comptes Rendus, 114, p.1510.

Ching-Hsie Yew and Goldsmith Werner (1964). "Stress distributions in soft metals due to static and dynamic loading by a steel sphere". Trans. ASME, J. App. Mech., Dec., 635-646.

Davies, R.M. (1949). "The determination of static and dynamic yield stresses using a steel ball". Proc. Roy. Soc., A197, p.416.

Engle Peter, A. (1976). "Impact Wear of Materials". Elsevier Scientific Publishing Co., New York.

Evans, A.G., Gulden, M.E. and Rosenblatt, M.E. (1978). Proc. Roy. Soc., London, Series A 361, p.343.

Flavenot, J.F. et Nikulari, A. (1977). La Mesure des Contraintes Residuelles: Methode de la (Fleche) Methode de la (Source de Contraintes). Les Memoires Techniques du CETIM (31).

Goldsmith, W. (1960). Impact, Arnold, London.

Goodier, J.N., Jahsman, W.E. and Rippenger, E.A. (1959). "An experimental surface-wave method for recording force-time curves in elastic impacts". J. App. Mech., 26, 3-7.

Halling, J. and Nuri, K.A. (1975). "Contact of rough surfaces of work-hardening materials". Proc. Symp. 1974 Int. Un. Theor. Applied Mechanics (IUTAM), Ed: A.D. de Paten and J.J. Kalker, Delft University Press.

Hardy, C., Baronet, C.N. and Tordion, G.V. (1971). Int. J. Numer. Methods Eng., 3, 451-462.

Hill, R. (1950). The Mathematical Theory of Plasticity, Oxford.

Hopkins, H.G. (1960). Progress in Solid Mechanics. Ed: I.N. Sneddon and R. Hill, Wiley (Interscience), New York, p.85.

Hutchings, I.M. (1979). "Energy absorbed by elastic waves during plastic impact". J. Phys. D. App. Phys., 12, 1819-1824.

Johnson, W. (1972). Impact Strength of Materials, Arnold, London.

Johnson, W. and Mellor, P.B. (1962). Plasticity for Engineers. Van Nostrand, London.

Kachanov, L.M. (1974). Fundamentals of the Theory of Plasticity. MIR Publishers, Moscow.

Kolsky, K. (1963). Stress Waves in Solids. Dover, New York.

Lamb, H. (1904). "On the propagation of tremors over the surface of an elastic solid". Phil. Trans. Roy. Soc., A203, 1-42.

Lowe, W.T., Al-Hassani, S.T.S. and Johnson, W. (1972). "Impact behaviour of small scale model motor coaches". Proc. I.Mech.E. Automobile Div., 186, 36, 409-419.

Meguid, S.A., Johnson, W. and Al-Hassani, S.T.S. (1976). "Some factors in the shot peening and peen-forming processes". Proc. 17th Int. Machine Tools Design & Research Conf., Birmingham, Sept., 3, 653-659, McMillans.

Merwin, J.E. and Johnson, K.L. (1963). "An analysis of plastic deformation in rolling contact". Inst. Mech. Eng., 177, 25, 676-685.

Pope, J.A. and Mohamed, A.K. (1975). "Residual plastic strain produced by single and repeated spherical impact". J. Iron & Steel Inst., July, 285-297.

Prandtl, L. (1920). Uber die Haerte plastischer Koerper, Nachten der Akademie der Wissenschaften Gotingen, Mathematisch-Physikalische Klasse, p.74.

Salem, S.A.L., Al-Hassani, S.T.S. and Johnson, W. (1975). "Aspects of the mechanics of driving nails into wood". Int. J. Mech. Sci., 17, 211-225.

Salem, S.A.L. and Al-Hassani, S.T.S. (1981). "Interfacial wave generation in explosive welding of multilaminates", Chapter 11, Shock Waves and High Strain-Rate Phenomena in Metals: Concepts and Applications". Eds: Marc. A. Meyer and Lawrence E. Murr, Plenum, New York.

Salem, S.A.L., Al-Hassani, S.T.S. and Johnson, W. (1979). "Measurements of surface pressure distribution during jet impact". Proc. 5th Int. Conf. "Erosion by Liquid and Solid Impact", Cambridge, U.K.

Samuels, L.E. and Mulhearn, T.O. (1957). "An experimental investigation of the deformed zone associated with indentation hardness impression". J. Mech. Phys. Solids, 5, p.125.

Shaw, M.C. and de Salvo, G. (1970). "A new approach to plasticity and its application to blunt two-dimensional indenters". Trans. ASME J. Eng. Industry, 92, 469-479.

Shaw, M.C. and de Salvo, G. (1970). "On the plastic flow beneath a blunt axisymmetric indenter". Trans. ASME J. Eng. Industry, 92, 480-493.

Silva Gomes, J.F. and Al-Hassani, S.T.S. (1977). "Internal fractures in spheres due to stress wave focusing". Int. J. Solids & Structures, 13, 1007-1017.

Tabei, A. (1981). M.Sc. Dissertation, Univ. Manch. Inst. Sci. Tech., U.K., Oct. 1981.

Tabor, D. (1951). The Hardness of Metals. Oxford Univ. Press.

Timoshenko, S. and Goodier, J.H. (1951). Theory of Elasticity. McGraw Hill, New York.

Tsai, Y.M. (1968). "Stress waves produced by impact on the surface of a plastic medium". J. Franklin Inst., 3, 204-221.

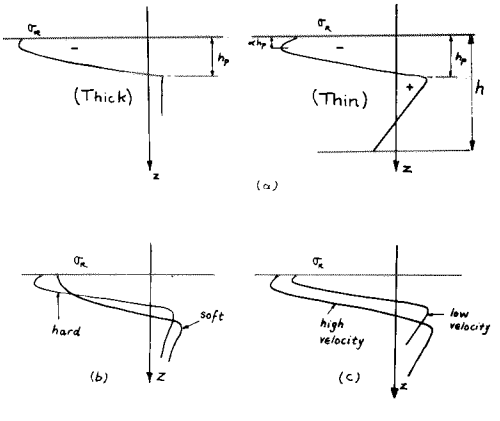

Fig. 1. Typical residual stress distributions.

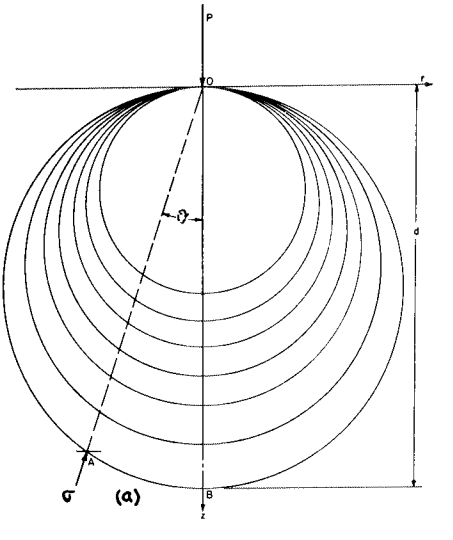

Fig. 2(a) Boussinesq solution for concentrated load P.

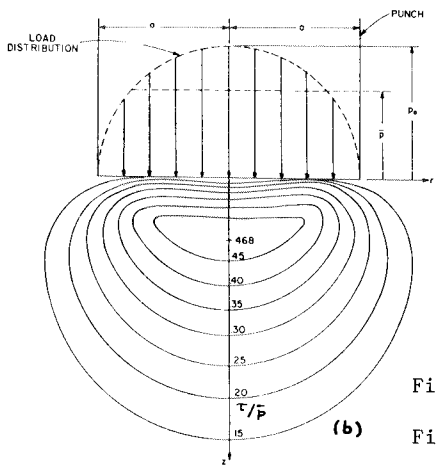

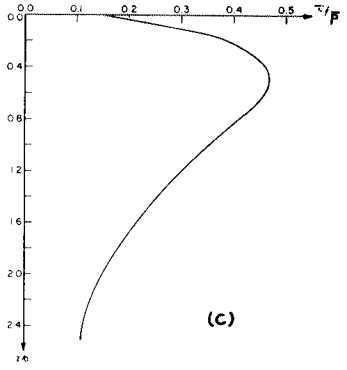

Fig. 2(b) Lines of constant $\tau/\bar{p}$ for smooth spherical indenter.

Fig. 2(c) $\tau/\bar{p}$ versus Z/a for vertical centre line (Shaw & de Salvo).

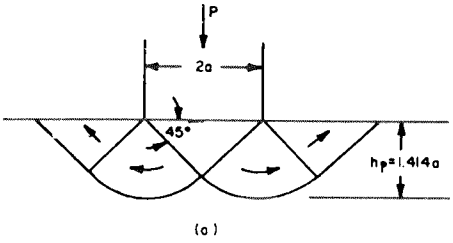

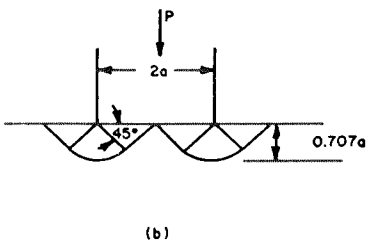

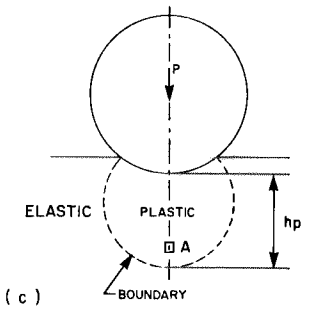

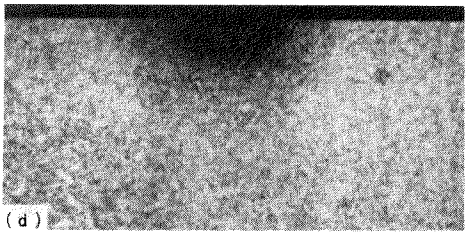

Fig. 3. Slip line flow fields (a) due to Prandtl, (b) due to Hill, (c) plastic/elastic boundary, (d) plastic zone after spherical projectile impact.

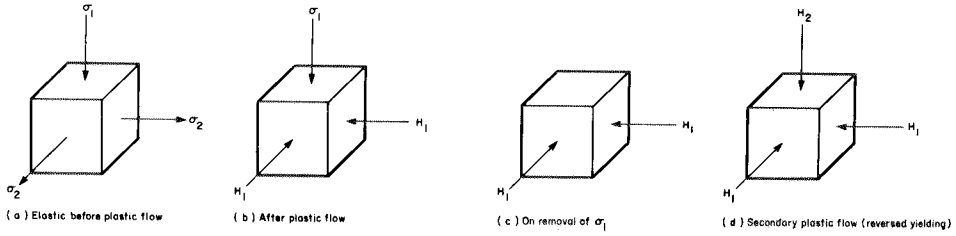

Fig. 4. Sequence of stress action in an element within the plastic zone.

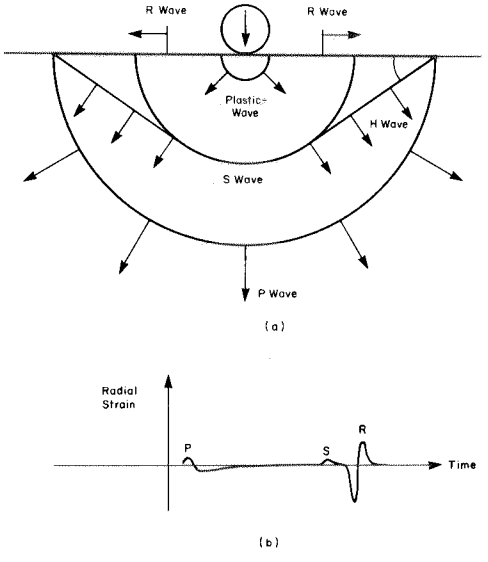

Fig. 5(a) Stress wave fronts commensurate during impact of a projectile on a semi-infinite solid. Fig. 5(b) A typical radial surface strain record at a position near the impact region.

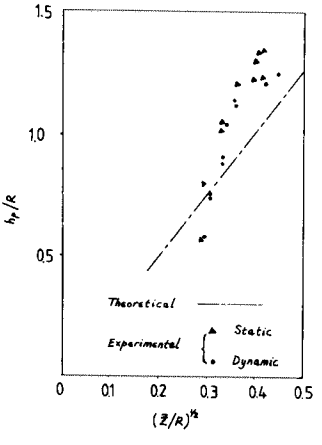

Fig. 7. Variation of h_p/R with $\bar{Z}/R$ for dynamic and static loading.

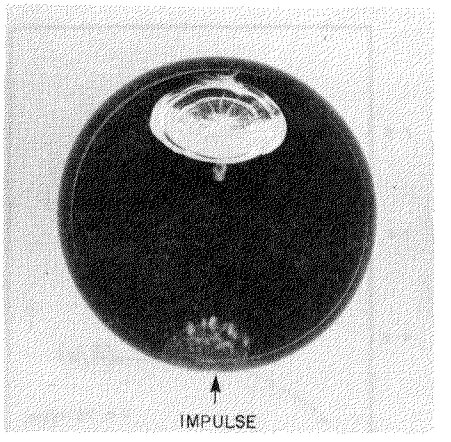

Fig. 6. Internal fractures in a Perspex sphere due to a point impulsive loading.

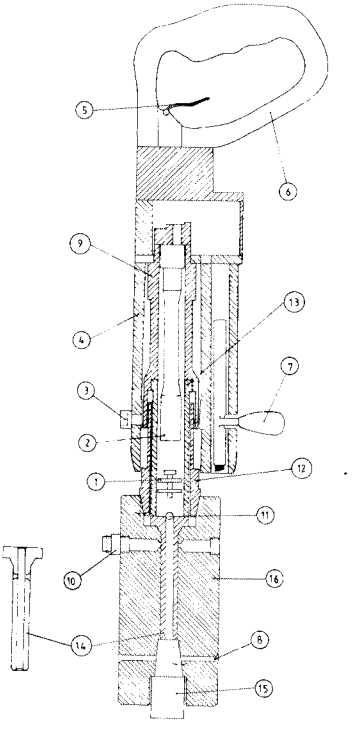

Fig. 8. Dynamic Test Rig. (1) Pin projectile. (2) Driver piston. (5) Firing pin. (10) Velocity measuring port holes. (11) Ball projectile. (14) Projectile Guide. (15) Target specimen.

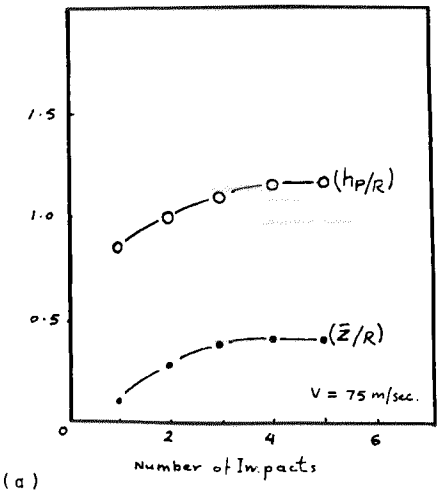

(a)

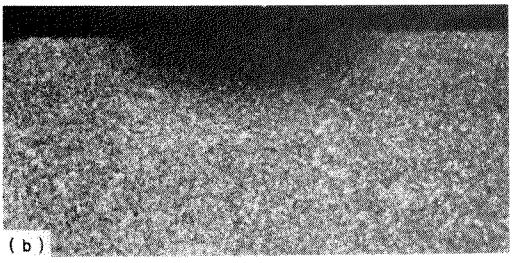

(b)

Fig. 9(a) Variation of h_p/R and Z/R with the number of impacts.
Fig. 9(b) Plastic zone overlap due to three adjacent impacts.

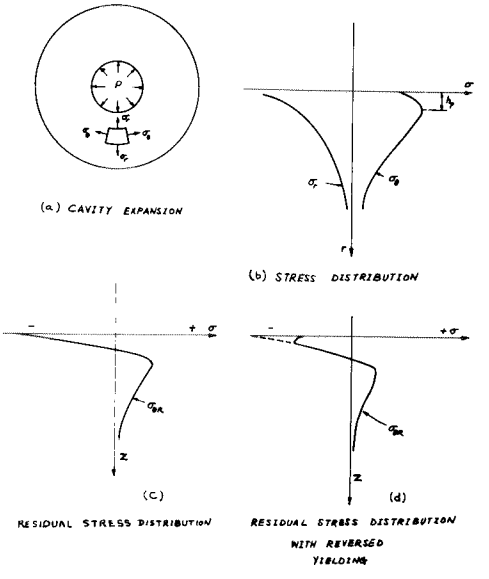

Fig. 10(a) Pressurized cavity model. (b) Radial and hoop stress in an elastic/plastic sphere. (c) Residual hoop stress distribution. (d) Residual stress distribution with reversed yielding.

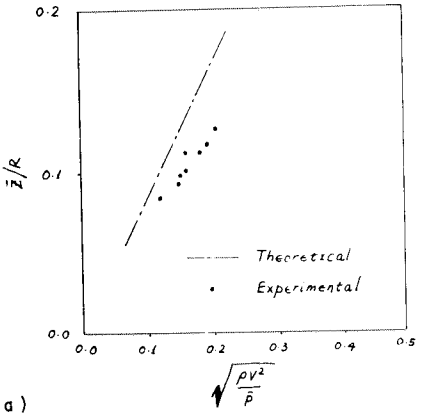

(a)

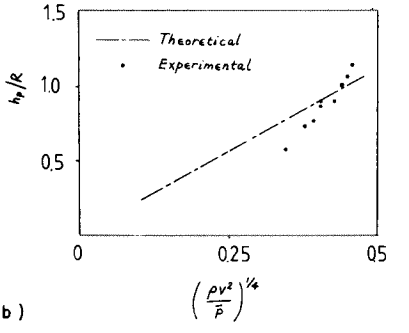

(b)

Fig. 11. Experimental and theoretical variation of (a) indentation $\bar{Z}$ and (b) depth of plastic zone h_p with the damage number.